Geometrical and Material Nonlinear Properties of Two-Dimensional Fabric Composites

Takashi Ishikawa,* Masamichi Matsushima,† and Youichi Hayashi*
National Aerospace Laboratory, Tokyo, Japan

The formerly developed nonlinear analysis of fabric composites is expanded to include longitudinal hardening in unidirectional carbon/epoxy composites and the deformed state in single-layer plain-weave composites. A simple constitutive equation is proposed to describe the hardening property. The full material nonlinear solution of the 8H satin carbon/epoxy system is in favorable agreement with the experimental results. It is confirmed that this material property is crucial in predicting a macroscopic behavior of fabric composites if warping is fully suppressed. An iterative procedure of the geometrical nonlinear analysis accounting for the warping is developed. The predicted stress-strain relations and warping coincide very well with the corresponding experimental results of carbon/epoxy plain-weave composites. The warping contributes greatly to the apparent hardening of this material at low stress levels.

Nomenclature

$A_{ij}(x), \bar{A}_{ij}$ = local and averaged in-plane stiffness
$a^*_{ij}(x), \bar{a}^*_{ij}$ = local and averaged in-plane compliance
a^{**}_{ij} = in-plane compliance in the warping-free state
a = width of a thread
a_u = length of a crimp part
$B_{ij}(x), \bar{B}_{ij}$ = local and averaged bending/stretching coupling stiffness
$b^*_{ij}(x), \bar{b}^*_{ij}$ = local and averaged bending/stretching coupling compliance
$D_{ij}(x), \bar{D}_{ij}$ = local and averaged bending stiffness
$d^*_{ij}(x), \bar{d}^*_{ij}$ = local and averaged bending compliance
h = thickness of a fabric composite plate
$h_1(x)$ = shape function of thread crimp
$h_2(x)$ = shape function of a warp section
h_t = thickness of a thread portion
N_i = membrane stress resultant
M_i = moment resultant
n_g = number of geometrical repeats in fabric structure
Q_{ij} = elastic stiffness matrix under plane stress
S_{ijkl} = higher order elastic compliance coefficients
W^* = a complementary energy function
$w(x)$ = local out-of-plane deformation (warping)
x,y,z = Cartesian coordinates
ϵ°_i = strain components at the geometrical midplane
κ_i = curvature at the geometrical midplane
$\theta(x)$ = local off-axis angle in fiber crimp
ν = Poisson's ratio

Superscripts

F = quantities of a fill thread
M = quantities of a pure matrix region
W = quantities of a warp thread
c = results of crimp model
f = quantities at the final state of deformation
i = quantities at ith loading step
s = results of bridging model

Received April 5, 1985; revision received Feb. 21, 1986.

*Senior Researcher, First Airframe Division. Member AIAA.
†Researcher, First Airframe Division.

Introduction

PRACTICAL applications of two-dimensional fabric composites are increasing in the area of advanced composite technology. Fabric reinforcements are employed in some composite airframes such as the Boeing 737 tailfins,[1] almost all parts of the Lear fan 2100,[2] and the Boeing 767 fairings.[3] Among those applications, the primary and subprimary structural members consist primarily of thicker panels with 4–10 or more plies and the secondary parts are constructed mainly with sandwich structures having thinner face sheets.

The widespread application of fabric composites and their linear mechanics have been discussed in the series of the publications by one of the authors.[4-6] The most important point in this mechanics is the local coupling effect between in- and out-of-plane deformation due to the interlacing structure in the fabrics. The macroscopic behavior of fabric composites is strongly governed by this effect. As a typical example, a clear dependency of the in-plane moduli of plain-weave carbon/epoxy is based on theoretical predictions.[7] The modulus increases with ply number and levels off at a value similar to that of multiple-layered 8H satin composites. The difference in the constraint of the local out-of-plane, or warping, deformation induces such a dependency. A restrictive state in the warping is, therefore, a crucial part of the linear mechanics of fabric composites. References 4–6 describe this linear aspect and the thermal responses.

A material nonlinear analysis of a local warp-free condition is included in Ref. 8. This analysis is oriented to the thicker panels used in aircraft applications. Very good agreement between the theory and experiments is reached for 8H satin glass/polyimide heat resistant composites.[8] For common 8H satin carbon composites, however, such a good correlation has not been found in some preliminary experiments. An investigation of the cause leads to a longitudinal nonlinear hardening of the material reported in a few papers.[9,10] The first part of this work is devoted to a treatment of this problem. A simple and reliable constitutive relation proposed by the authors[11] is adopted here and a great improvement is achieved in the correlation.

A single-layer membrane structure of carbon/epoxy fabrics under pretensile loads is regarded as a possible candidate for spacecraft solar paddles. A plain-wave fabric must be chosen in order to avoid a macroscopic thermal warping.[4] Some preliminary vibration tests clarify a serious nonlinear hardening exceeding that in a common membrane.[12] This

phenomenon can be attributed to the nonlinear stress-strain relationship in such a single-layer weave composite. However, the longitudinal material behavior mentioned above does not account for the hardening at a low stress level.

The second part of the present paper treats this problem by introducing a geometrical nonlinear analysis. Essentially, an iterative description of the deformed shape in the x-z plane is required. The sources of material nonlinear behavior are also incorporated in the theoretical procedure. Stress-strain relationships and local warping values are experimentally obtained using some optical devices and compared to the theory. Contributions of geometrical and material nonlinearities to the macroscopic behavior are basically identified for the present material system. This comparison is also consistent with a very small elastic modulus of the plain weave carbon/epoxy with one ply at a low stress level reported in Ref. 7.

Basic Concepts and Material Nonlinear Analysis

Basis of the Theory and Crimp Model

The pure elastic part of the present theory has been published in previous papers[4,5] and, hence, duplication is avoided here as much as possible. The description of the constitutive equation of classical lamination theory is omitted. We will follow the regular definitions of stiffness, compliance coefficients, etc., of Ref. 13.

An important condition about the suppression of the out-of-plane deformation, or warping, should be stated. If any warping is not allowed, the following equations must hold:

$$\{\kappa_i\}=0,\ \{M_i\}\neq 0 \tag{1}$$

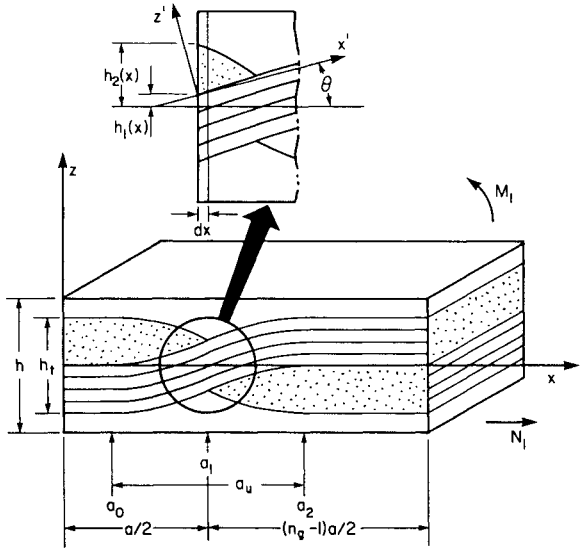

a) Crimp model.

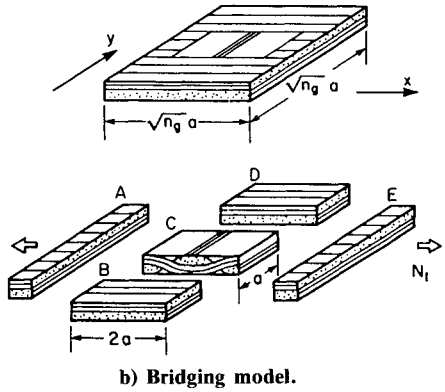

b) Bridging model.

Fig. 1 Geometry of mechanical models.

These conditions lead to the one-to-one inversion relation between A_{ij} and the bending-free compliance a_{ij}^{**} as

$$[a_{ij}^{**}]=[a_{ij}^{*}]-[b_{ik}^{*}][d_{kl}^{*}]^{-1}[b_{ij}^{*}]=[A_{ij}]^{-1} \tag{2}$$

Equation (2) indicates that the coupling terms no longer make sense or, in other words, that the material distribution along the z axis does not affect an in-plane response. The present local warping constrained and the opposing local warping allowed conditions are abbreviated below as LWC and LWA respectively.

Descriptions of the one-dimensional crimp and two-dimensional bridging models appear in Refs. 4-6. An illustration of the crimp model is given in Fig. 1a where the sinusoidal shapes of the crimp, h_1 and h_2, are postulated. The following assumption is introduced first. The lamination theory is valid in an infinitesimal slice with the length of dx. Then, we can define local stiffness coefficients, $A_{ij}(x)$, $B_{ij}(x)$, and $D_{ij}(x)$, with the knowledge of the material distribution along the z axis. By inverting the local stiffness coefficients of a 6×6 matrix, we have the local compliance coefficients. If we consider the crimp model under an in-plane force N_1, a uniform distribution of N_1 along the x axis can be expected. Hence, the averaged in-plane compliance can be calculated for the LWA state as

$$\bar{a}_{ij}^{*c}=\frac{2}{n_g a}\int_0^{n_g a/2} a_{ij}^{*}(x)\,dx$$

$$=\left(1-\frac{2a_u}{n_g a}\right)a_{ij}^{*}+\frac{2}{n_g a}\int_{a_0}^{a_2} a_{ij}^{*}(x)\,dx \tag{3}$$

where the superscript c denotes the result of the crimp model. In order to obtain the solution for the LWC state, $a_{ij}^{*}(x)$ should be replaced by $a_{ij}^{**}(x)$, which can be determined by the simple inversion of a 3×3 matrix of $A_{ij}(x)$.

Nonlinear Analysis of the Crimp and the Bridging Models

The material nonlinear analysis is conducted[8] for this model by incorporating the nonlinear stiffness matrix with the description of the local stiffness coefficients. The first material behavior taken into account is the transverse failure normal to the loads. A simple "knee type" analysis[15] is employed for the cracked region where the strain exceeds the specified value ϵ_2^b.

The second material property is related to the nonlinear off-axis behavior induced by the pure shear response.[16] An off-axis angle due to the thread crimp θ in Fig. 1a is the cause of such behavior. By employing the higher-order compliance used in Ref. 16, we can describe the nonlinearity in the fill thread. Nonlinear behavior of the neat matrix region is the third property treated in the present analysis in a manner similar to the off-axis nonlinearity.

An iterative procedure inevitable in most nonlinear calculation is also required here. The controlled stress scheme where N_1 is specified is utilized according to the nature of the model. The nonlinear stiffness matrices are introduced at a given location of the crimp model if necessary. Then, the local nonlinear compliance matrix $a_{ij}^{*\prime}(x)$ is obtained. A prime indicates the nonlinear state. The average of $\bar{a}_{ij}^{*\prime c}$ is next calculated from Eq. (3). Based upon the initial value of N_1 and this result, we have an averaged $\bar{\epsilon}_1^{\circ}$ for the entire model. This procedure consists of one closed loop in the actual computation. The difference between the initial $\bar{\epsilon}_1^{\circ}$ and the revised one is denoted by $\Delta\bar{\epsilon}_1^{\circ}$. For terminating the iterative loop, the following condition is imposed:

$$|\Delta\bar{\epsilon}_1^{\circ}/\bar{\epsilon}_1^{\circ}|\leq 1.0\times 10^{-3} \tag{4}$$

Some other precautions are necessary for selecting numerical parameters and details have been presented in Ref. 8. Numerical results are shown later in the discussion section.

Given below is a brief note about how the bridging model shown in Fig. 1b analyzes the material nonlinear behavior of 8H satin composities. In practical applications, a single-layer plate of 8H satin is never used because it exhibits significant thermal warping.[4] Semisymmetrical lamination of multiple plies is needed; hence, it follows that the LWC solution is compatible with this model. By assuming the load distribution in the surrounding regions of the crimp portion (B, C, and D in Fig. 1b), we obtain an averaging formula of stiffness. We should use the LWC version of the theory for further developments according to the aforementioned fact. Descriptions of detailed equations are given in Ref. 8.

The three nonlinear material properties mentioned above can be similarly incorporated into the present model. It should be noted that warp threads in the regions B and D (or A and E) fail simultaneously owing to the simple knee treatment. Hence, linear stress-strain relations will be obtained after such failures unless the off-axis and neat resin nonlinearities are taken into account. The LWC numerical results for a heat-resistant glass/polyimide material with 8H satin reinforcements are illustrated in Ref. 8. The theoretical predictions are in a very good agreement with the experiments on 16-ply specimens. for the case of 8H satin carbon/epoxy, however, the analysis including such properties alone does not provide a satisfactory correlation. Thus, the following type of nonlinearity is investigated by the authors.

Longitudinal Material Behavior of UD Carbon Composites

It is not well known that the unidirectional (UD) carbon composites exhibit significant hardening in longitudinal tension. The experimental results in Refs. 9 and 11 are compared in Fig. 2. The longitudinal modulus at a higher stress level can be 20% larger than at the zero stress value. The analogous behavior of single carbon fibers is reported in Ref. 18 and a linear relation between the stress and longitudinal modulus of composites is proposed in Ref. 9, as plotted in Fig. 2. Recently, a rational approach[10] has been conducted for such a non-Hookean property, although it is not fully appropriate to the present problem. An alternative constitutive equation is proposed in Ref. 11, where the compliance coefficients of higher orders (similar to those in Ref. 16) are introduced. This approach is simple and easy to apply despite its theoretical soundness.

The existence of a complementary energy function W^* is assumed first, which is consistent with the reversible nature of the present behavior. Employing a polynomial expansion of W^* up to fourth order and considering a longitudinal uniaxial tensile state results in the expression of the strain in this direction,

$$\epsilon_1 = \frac{\partial W^*}{\partial e_{11}} = S_{11}\sigma_1 + S_{111}\sigma_1^2 + S_{1111}\sigma_1^3 \tag{5}$$

Hence, the elastic modulus is described by a fractional function of the stress of a second order, such as

$$E_L = \frac{d\sigma_1}{d\epsilon_1} = \frac{1}{d\epsilon_1/d\sigma_1} = \frac{1}{S_{11} + 2S_{111}\sigma_1 + 3S_{1111}\sigma_1^2} \tag{6}$$

Comparing and fitting Eq. (6) with the experimental results in Fig. 2 brings a determination procedure of S_{11}, S_{111}, and S_{1111}. The following result of Ref. 11 is adopted here:

$$E_L = \frac{1000}{7.634 - 2.444\sigma_1 + 1.111\sigma_1^2} \text{ GPa} \tag{7}$$

Note that Eq. (7) also agrees well with the compressive longitudinal moduli.[11] A transformation calculation of a macroscopic stress into the local coordinate system with θ is required in the actual application of Eq. (7) to the crimp model. The determined strain by Eq. (7) in the local coordinate is retransformed into the global system. Numerical results are indicated in the discussion section.

Geometrical Nonlinear Analysis

Background

A practical need for the nonlinear analysis of single-layer plain-weave composites of carbon/epoxy has arisen recently. These materials show remarkable nonlinear responses at low tensile stress, as indicated later in Fig. 5. Certain preliminary calculations reveal that the aforementioned longitudinal behavior is not sufficient for a complete description. An observation of surfaces of the specimens under tensile loads suggests qualitatively that the warping deformation can be included.

A consideration of the geometrical nonlinear behavior is a key factor for solving this problem. A step-by-step description of the deformed shape due to the local coupling effect is carried out and, hence, the LWA condition is assumed a

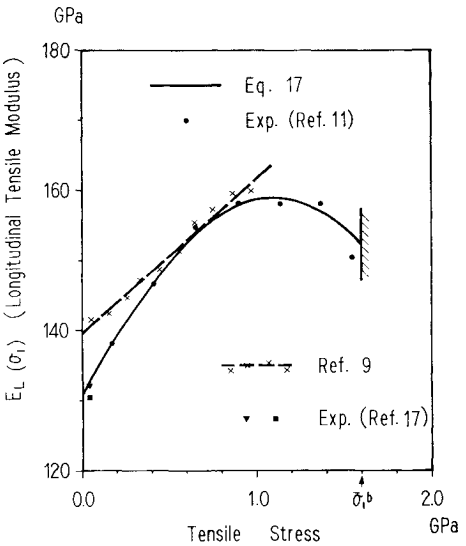

Fig. 2 Longitudinal modulus of unidirectional composites dependent on tensile stress.

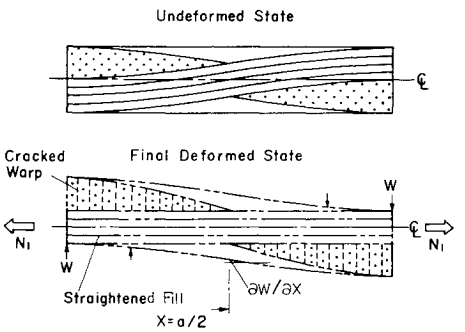

Fig. 3 Situation of straightening with the warping deformation.

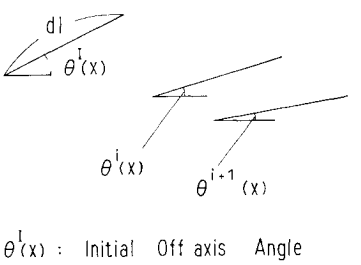

Fig. 4 Rigid-body rotation of an infinitesimal line element.

priori. Further considerations of geometrical nonlinear effects such as a distinction between Green and Almansi strain tensors are omitted here. The four nonlinear material properties are preserved in the framework of this part of the theory.

Formulation

A schematic illustration of this problem is given in Fig. 3. Let us consider an increment of the in-plane stress resultant at the ith step, ΔN_1^i, applied to the crimp model of Fig. 1a or 3. Mathematical expressions should be written with respect to an immobile point during a loading process. The center of symmetry of $x=a/2$ and $z=0$ can be postulated as such a point by considering a periodic structure. By using the constitutive relation of lamination theory, we have the following local curvature:

$$\frac{-\Delta\partial^2 w^i}{\partial x^2}=\kappa_1^i(x)=b_{11}^*(x)^i\Delta N_1^i \tag{8}$$

This equation is also a re-entry point of the actual iterative calculation. Then, we can determine a decrease of the local off-axis angle $\Delta\theta^i$ by an integration

$$\Delta\theta^i(x)\simeq\Delta\left(\frac{\partial w^i}{\partial x}\right)=\int_0^x b_{11}^*(\xi)^i\Delta N_1^i\,\mathrm{d}\xi \tag{9}$$

Here, we utilize the boundary condition that $\theta(0)=0$, which always holds be virtue of the symmetry. A variation in θ naturally affects the fill stiffness $Q_{ij}^F(\theta)$, although later the extent turns out to be small. Next, we obtain the expression of the increment of the warping as follows:

$$\Delta w^i(x)=\int_{a/2}^x \Delta\theta^i(\xi)\mathrm{d}\xi \tag{10}$$

where the aforementioned immobility at $x=a/2$ is considered. An accumulated value of the warping is then calculated with the knowledge of the warping at the previous loading step, $w^{i-1}(x)$

$$w^i(x)=w^{i-1}(x)+\Delta w^i(x) \tag{11}$$

This result is used as the initial value of the iteration at each ith step. Such warping deformation has an influence upon the local coupling and bending coefficients, whereas $A_{ij}(x)$ is not affected. As an example, a modified coupling coefficient by $w^i(x)$, $B'_{ij}(x)$, is written for $0\le x\le a/2$

$$\begin{aligned}B'_{ij}(x)=&\int_{-h/2+w^i(x)}^{h_1(x)-h_t/2+w^i(x)} Q_{ij}^M z\cdot\mathrm{d}z\\&+\int_{h_1(x)-h_t/2+w^i(x)}^{h_1(x)+w^i(x)} Q_{ij}^F(\theta)z\cdot\mathrm{d}z\\&+\int_{h_1(x)+w^i(x)}^{h_2(x)+w^i(x)} Q_{ij}^W z\cdot\mathrm{d}z+\int_{h(x)+w^i(x)}^{h/2+w^i(x)} Q_{ij}^M z\cdot\mathrm{d}z\end{aligned} \tag{12}$$

where $h_1(x)$, etc., are the shape function of the crimp.[14] These modifications of $B'_{ij}(x)$ and $D'_{ij}(x)$ induce variations in $a_{ij}^*(x)$, $b_{ij}^*(x)$, and $d_{ij}^*(x)$; hence, $b_{11}^*(x)$ in Eq. (8) must be rewritten. Thus, a loop from Eq. (8) to Eq. (12) is formed and a convergent criterion similar to Eq. (4) is introduced. The next $i+1$th step is started after a converged strain is obtained.

It is interesting and instructive to examine the final deformed state of Fig. 3b. If we admit that $Q_{ij}^W\simeq 0$ due to the extended transverse cracks and assume that Q_{ij}^M can be neglected, the following form of the warping is easily derived in order that the coupling term vanishes everywhere along the x direction:

$$w^f(x)=\frac{h_t}{4}-h_1(x)=-\frac{h_t}{4}\cdot\sin\left[\left(x-\frac{a}{2}\right)\cdot\frac{\pi}{a}\right] \tag{13}$$

or

$$w^f(x)+h_1(x)=h_t/4 \tag{14}$$

where $a=a_u$ is assumed and superscript f denotes the final state. Equation (14) indicates that the fill thread is competely straightened in the final deformed shape. Hence, $b_{ij}^{*\prime}(x)$ also vanishes and no more warping occurs, as indicated in Eqs. (8-11). This state provides a higher in-plane modulus than the initial LWA solution. If we assume the cylindrical bending state, a simple explanation can be shown here. An in-plane compliance in this state can be written as

$$a_{11}^*(x)=\frac{D_{11}(x)}{A_{11}(x)\cdot D_{11}(x)-B_{11}(x)^2} \tag{15}$$

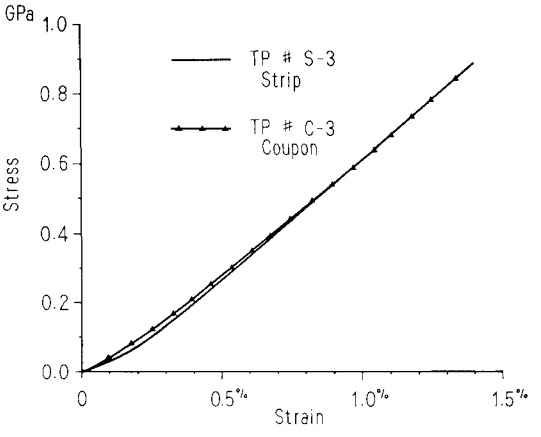

Fig. 5 Examples of measured stress-strain relations of strip and coupon specimens made of carbon/epoxy plain weave composites with a single ply (TP = test piece number).

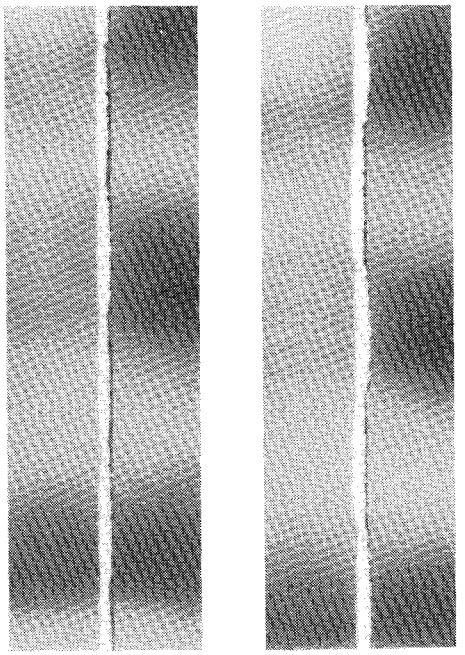

a) $\sigma_1=0.027$ GPa. **b) $\sigma_1=0.728$ GPa.**

Fig. 6 Magnified sectional views of a strip specimen under two levels of tensile stress.

It follows that $a_{11}^{*}(x)$ tends to the simple inverse of $A_{11}(x)$ because of the vanishing $B_{11}(x)$. This mechanism is fundamental in the geometrical hardening of the plain composites with a single ply. Therefore, a measurement of $w^{i}(x)$ is conducted and stated later.

The effect of a rigid-body rotation derived by the straightening should be taken into account. Figure 4 is provided for a conceptual illustration of this phenomenon. We consider a rigid infinitesimal line element subjected to the variation of θ. As implied earlier, we adopt the Lagrangian description of the deformed state here. Hence, the following expression of the strain component in the x direction can be obtained between ith and $i+1$ loading steps:

$$\Delta\epsilon_{rr}^{i}(x)=\frac{\cos[\theta^{i+1}(x)]-\cos[\theta^{i}(x)]}{\cos[\theta(x)]} \tag{16}$$

where subscript rr signifies the rigid-body rotation. The extent of this effect turns out to be secondary at the later state.

Comments on Bending Deformation Related to Material Behavior

All of the material nonlinear stiffness matrices are substituted for Q_{ij}^{M}, etc., in Eq. (12) and in omitted equations for $A_{ij}^{\prime}(x)$ and $D_{ij}^{\prime}(x)$. A particular consideration of the induced bending deformation is necessary in the LWA state. In the previous LWC case, a strain distribution in the thickness direction is uniform owing to the assumptions of classical lamination theory, whereas it should be determined first in the present case. The linear function to z is introduced based on the assumption

$$\Delta\epsilon_{1}(z)=\Delta\epsilon_{1}^{\circ}+z\cdot\Delta\kappa_{1}=(a_{11}^{*}+z\cdot b_{11}^{*})\cdot\Delta N_{1} \tag{17}$$

A typical usage of Eq. (17) is a treatment of the knee behavior. It is required to determine the height h_3, where the strain reaches the critical value ϵ_2^{b} as follows:

$$h_3(x)=h_2=(h_2-h_1)\frac{\epsilon_2(h_2)-\epsilon_2^{b}}{\epsilon_2(h_2)-\epsilon_2(h_1)},\quad 0\le x\le\frac{a}{2} \tag{18}$$

where $\epsilon_2(h_2)$ denotes the strain at the upper edge of the warp and it is larger than ϵ_2^{b}. Then, the local in-plane stiffness for the region containing the partly damaged warp in given as

$$\begin{aligned}A_{ij}(x)&=Q_{ij}^{M}[h_1(x)-h_2(x)+h-h_t/2]\\&+Q_{ij}^{F}(\theta)h_t/2+Q_{ij}^{W}[h_3(x)-h_1(x)]\\&+Q_{ij}^{\prime W}[h_2(x)-h_3(x)],\quad 0\le x\le a/2\end{aligned} \tag{19}$$

Greater details on this procedure is presented in Ref. 14. In the case of Q_{ij}^{M} and $Q_{ij}^{F}(\theta)$, the variation of these stiffness is continuous along the z axis. Therefore, they are evaluated at certain discrete points and numerically integrated in the thickness direction. Again, all of the numerical results of this section are presented later.

Experiments

Some experiments are carried to obtain nonlinear stress-strain responses of carbon/epoxy fabric composites. Two material systems are selected consistent with the theoretical approaches: 1) an 8H satin composite with four plies cured semisymmetrically[4] and 2) a single-layer plain composite. The former consists of 1K-AS fibers and 410 epoxy resin comparable to 5208 and the latter of 6K-T 500 fibers and a certain epoxy. The thread densities in the fill and warp directions are almost identical for both fabrics. The averages of V_f are 63% for the 8H satin and 67% for the plain.

Strip specimens containing only one thread and regular coupon specimens are both used for the plain weave. A nominal width of the strip is 3 mm and that of the coupon 20 mm. Coupon specimens of 8H satin are 12.5 mm wide and the difference in the widths reflects the thread sizes. The lengths of all the specimens are almost 300 mm.

We cannot rely on common strain gages because some specimens are very thin. Therefore, a pair of electro-optical transducers are utilized here as an extensometer. This device works very well with a longer gage length of 100 mm and under appropriate experimental techniques. An Instron 1125 universal testing machine is used for loading. Acoustic emission signals are also monitored and processed in certain specimens through a wide-band sensor.

Two examples of the acquired stress-strain data are shown in Fig. 5 for the single-layer plain system. The shapes of the curves are rather similar and, hence, the existence of the neighboring threads is less influential than the neighboring layers.[7]

The induced warping by tensile loads is measured for the plain-weave specimens. Magnified photographs and a replication technique through acetyl cellulose films are both employed. Magnified sectional views of a strip specimen (S-4) under two levels of tensile stress are shown in Fig. 6. The warping is easily identified; and it is understood that the illustration of Fig. 3 is quite close to the real situation. A diagram and a picture of the measuring system is given in Fig. 7. Note the two telescopes of the transducers and the camera.

Comparisons of Numerical and Experimental Results and Discussion

LWC Solutions for 8H Satin

Input data for numerical calculations are listed in Table 1 corresponding to the two material systems. The values in Ref. 8 and Eq. (17) are chosen as the nonlinear material coefficients. Geometrical parameters in the shape of the crimp are so determined that the actual shape is close to the assumed one.

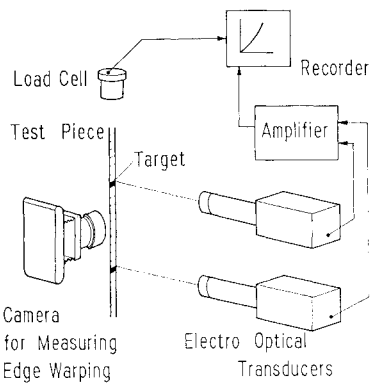

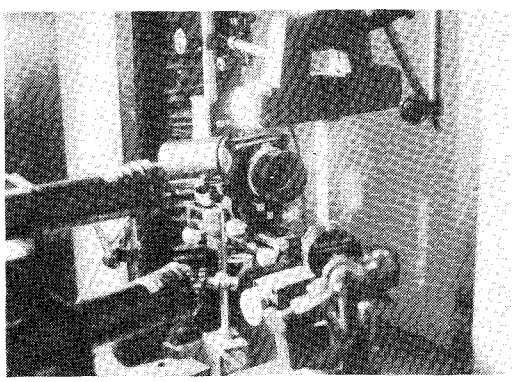

Fig. 7 Measurement system of the warping and longitudinal behavior for the plain-weave fabric composites.

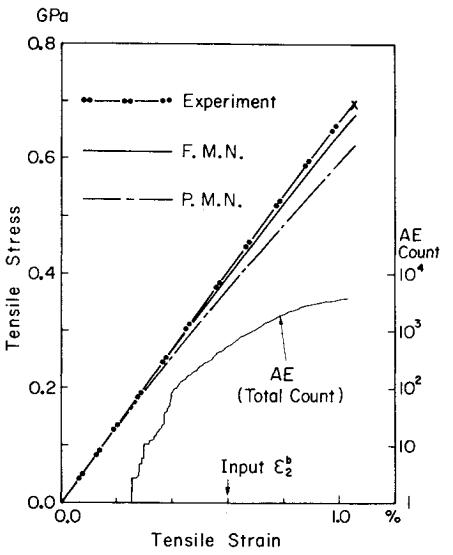

Fig. 8 Theoretical and experimental stress-strain relations of 8H satin carbon/epoxy composites (FMN = fully material nonlinear solution including longitudinal nonlinearity, PMN = partially material nonlinear solution with three constitutive properties).[8]

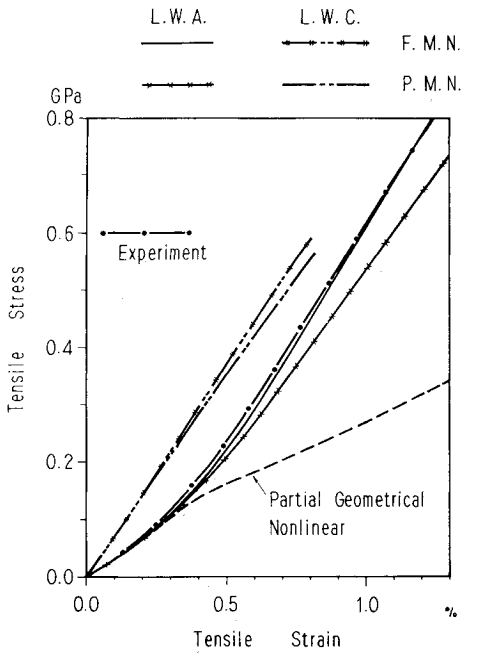

Fig. 9 Theoretical and experimental stress-strain relations of single layer carbon/epoxy plain composites (LWA = local warping allowed solution, LWC = local warping constrained solution).

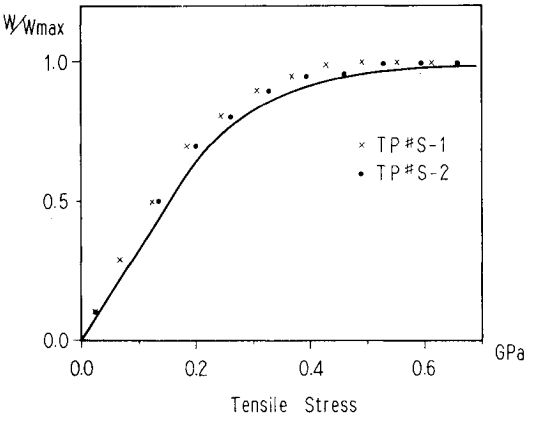

Fig. 10 Relationships between nondimensionalized induced warping and tensile stress in the strip specimens for comparison of the theory and experiments.

Figure 8 is shown first for the correlation between theory and experiments of the 8H satin material. A solid line denotes the fully material nonlinear (FMN) solution where the four sources of nonlinearities are included. The partial nonlinear (PMN) solution without the longitudinal behavior is indicated by a chain line. An experimental stress-strain relation is shown by a double chain line and a relation of the AE total count vs strain is also plotted.

An agreement between the FMN and experimental results is very favorable in the entire region of the stress, while the PMN solution departs from other curves at higher stress levels. The reason can be attributed to the larger crimp ratio of $h/a = 0.35$ in this material, which induces more nonlinear shear strain. The AE total count is related mainly to the transverse cracking, which is less influential for carbon than glass composites owing to a relative dominance of the longitudinal moduli. These cracks start much earlier than the input ϵ_2^b and are caused by a certain strain concentration around a wedge-shaped edge of the warp.[14] We can summarize that nonlinear hardening is the dominant property and its inclusion allows better prediction.

A short comment on the geometrical nonlinear solution for the present case is given here. Because the warping is suppressed completely, a finite displacement in the x direction is the only possible cause of the geometrical nonlinearity. The consideration of this factor, however, results in a trivial deviation from the previous solutions. Hence, this effect is omitted for the LWC case.

LWA Solutions for Plain Weave

Experimental and theoretical results are compared in Fig. 9. The experimental data of a strip specimen (S-2) is selected as a typical example and indicated by a chain line. It should be noted that the one-dimensional state assumed in the analysis is almost realized in the strip specimens.

A pure solid line showing the best agreement with the experimental curve indicates the solution in the LWA state with the full material nonlinearities. A solid curve with crosses denotes the PMN solution explained above and again departs from the experimental result. A dashed line signifies the partial geometrical nonlinear result where the effects of the variation of the local off-axis angle related to Eqs. (9) and (16) are included. In the present LWA case, a sole consideration of this factor results in an erroneous solution. A pair of curves in the FMN and PMN cases under the LWC

Table 1 Linear and nonlinear material properties of unidirectional carbon/epoxy composites and crimp parameters of fabrics

E_L $(=1/S_{11})$	131.0 GPa	
E_T	10.8 GPa	
G_{LT}	5.20 GPa	
ν_L	0.26	
ν_{TT}	0.46	
S_{111}	$-1.222\ 10^{-3}$ GPa^{-2}	
S_{1111}	$0.3703\ 10^{-3}$ GPa^{-3}	
ϵ_2^b	0.6%	
E_m	4.51 GPa	
ν_m	0.38	
S_{1111}^M	9.88 GPa^{-3}	
	8H Satin	Plain
$h = h_t$, mm	0.35	0.25
$a = a_u$, mm	1.0	3.0

condition show a considerable discrepancy from the experiment, whereas they provide similar tangents to the LWA result at a higher stress level.

By comparing all of the indicated results, we can summarize the following points for this material system. An initial low stiffness (which is also demonstrated in Fig. 5 for the coupon specimen) is caused by the allowed warping. This fact is consistent with the dependency of the elastic modulus upon a ply number reported in Ref. 7 and it is again confirmed in Fig. 1a. The straightening produces a higher modulus at a middle level of stress resulting a macroscopic hardening. The longitudinal material behavior has some influence upon the final state of the stress-strain relations.

It is necessary to examine the contributions of the two factors of the geometrical nonlinearity. At $\sigma=0.2$ GPa, the total strain and the contribution of the rigid-body rotation are 0.47 and 0.09%, respectively, for the present LWA/FMN case, while the vanishing of the local coupling produces a 0.12%. Thus, the rigid-body rotation seems to be secondary, as mentioned earlier. It is quite insufficient to include only the effect of the local off-axis angle in the theory.

Figure 10 compares the predictions and measured values of nondimensionalized warping. The solid line signifies the theoretical values of $w^i(0)/(h_t/4)$ obtained from Eq. (11) and the material properties of Table 1. The correlation between the theory and experiments is very favorable. We can observe that 80% of the warping is already induced by 0.3 GPa, where the initial serious hardening is almost over. Thus, the previous understanding of the mechanism of hardening is directly verified.

Conclusions

1) The formerly developed material nonlinear analysis of fabric composites is extended in two aspects: one is a consideration of the longitudinal material behavior for carbon fabrics and the other a description of the geometrical nonlinearity.

2) A fractional constitutive equation with a quadratic denominator of the stress is derived based on the theory of nonlinear elasticity for describing the longitudinal property of unidirectional carbon composites.

3) A significant improvement is realized by introducing such an equation into the correlation between theory and experiment for nonlinear stress-strain relations of 8H satin composites. The partial material nonlinear solution without the longitudinal behavior deviates considerably from the experimental curve at higher stress levels. The material nonlinear properties are most crucial in the prediction of the macroscopic behavior when the local warping deformation is almost completely suppressed.

4) A theoretical procedure is developed in order to incorporate the description of the deformed state into the analysis of the apparent hardening of the single-layer plain-weave composites. The change in the local off-axis angle, the warping making the local coupling terms smaller, and the effect of the rigid-body rotation are taken into account. The former nonlinear material properties are preserved in the procedure.

5) It is both theoretically and experimentally confirmed that the early hardening is caused by the allowance of the local warping. The fully nonlinear solution in terms of both material and geometrical aspects coincide fairly well with the experimental result of a strip specimen. The measured warping values are in good agreement with the theoretical predictions. The longitudinal material behavior becomes significant in the later region of the stress-strain relations. This finding is compatible with the dependency of elastic modulus of plain-weave composites upon the number of plies discovered by the authors.

6) The geometrical nonlinear description is essential for analyzing the apparent hardening behavior when the local warping is almost allowed. A clarification of such behavior of the single-layer plain carbon/epoxy system is quite significant in practice for the application of this material to space tension structures.

Acknowledgment

The authors wish to thank Professor T. W. Chou of the University of Delaware for his encouragment in the earlier part of this work. They also express their sincere graditude to Messrs. Y. Nakajima and K. Ito for significant contributions to the experimental effort.

References

[1]McCarty, J. E., Johnson, R. W., and Wilson, D. R., "737 Graphite-Epoxy Horizontal Stabilizer Certification," *Proceedings of the AIAA 23rd Structures, Structural Dynamics and Materials Conferences*, Part 1, New Orleans, LA, May 1982, pp. 307-322.

[2]Wigotsky, V., "First Design Details of the All-Composites Lear Fan," *Astronautics & Aeronautics*, Vol. 21, May 1983, pp. 30-32.

[3]Ono, D., "Application of Composite Materials in Aerospace Industries," *Promoting Machine Industry in Japan*, Vol. 16, June 1983, pp. 20-25 (in Japanese).

[4]Ishikawa, T., "Anti-Symmetric Elastic Properties of Composite Plates of Satin Weave Cloth," *Fibre Science and Technology*, Vol. 15, Sept. 1981, pp. 127-145.

[5]Ishikawa, T. and Chou, T. W., "One-Dimensional Micromechanical Analysis of Woven Fabric Composites," *AIAA Journal*, Vol. 21, Dec. 1983, pp. 1714-1721.

[6]Ishikawa, T. and Chou, T. W., "In-Plane Thermal Expansion and Thermal Bending Coefficients of Fabric Composites," *Journal of Composite Materials*, Vol. 17, No. 2, March 1983, pp. 92-104.

[7]Ishikawa, T., Matsushima, M,, Hayashi, Y., and Chou, T. W., "Experimental Confirmation of the Theory of Elastic Moduli of Fabric Composites," *Journal of Composite Materials*, Vol. 19, No. 5, Sept. 1985, pp. 443-458.

[8]Ishikawa, T. and Chou, T. W., "Nonlinear Behavior of Woven Fabric Composites," *Journal of Composite Materials*, Vol. 17, No. 5, Sept. 1983, pp. 399-413.

[9]van Dreumel, W.H.M. and Kamp, J.L.M., "Non-Hookean Behavior in the Fibre Direction of Carbon-Fibre Composites and the Influence of Fibre Waviness on the Tensile Properties," *Journal of Composite Materials*, Vol. 11, No. 4, Oct. 1977, pp. 461-469.

[10]Pindera, M.-J. and Herakovich, C. T., "An Elastic Potential for the Nonlinear Response of Unidirectional Graphite Composites," *Journal of Applied Mechanics*, Vol. 51, No. 3, Sept. 1984, pp. 546-550.

[11]Ishikawa, T., Matsushima, M., and Hayashi, Y., "Hardening Nonlinear Behavior in Longitudinal Tension of Unidirectional Carbon Composites," *Journal of Materials Science*, Vol. 20, Nov. 1985, pp. 4075-4083.

[12]Kibe, S., Kai, T., Hanawa, T., Tanizawa, K., Imura, N., and Ogata, Y., "Developments of Membrane Structure Under Tension and Its Vibration Propeties," *Proceedings of 28th Space Sciences and Technology Conference*, Japan Society of Space and Aeronautical Sciences, Oct. 1984, pp. 566-567 (in Japanese).

[13]Jones, R. M., *Mechanics of Composite Materials*, McGraw-Hill Book Co., New York, 1975.

[14]Ishikawa, T. and Chou, T. W., "Stiffness and Strength Behavior of Woven Fabric Composites," *Journal of Materials Science*, Vol. 17, Nov. 1981, pp. 3211-3220.

[15]Tsai, S. W., "Strength Characteristics of Composite Materials," NASA CR-224, April 1965.

[16]Hahn, H. T. and Tsai, S. W., "Nonlinear Elastic Behavior of Unidirectional Composite Laminae," *Journal of Composite Materials*, Vol. 7, Jan. 1973, pp. 102-118.

[17]Nakamichi, J., Noguchi, Y., and Ishikawa, T., "Verification of a Computer Program for Vibration Analysis of Composite Wing Cores," National Aerospace Laboratory, Tokyo, TR-825, July 1984 (in Japanese).